doi:10.1093/brain/awq043 Brain 2010: 133; 1224–1238 | 1224

BRAIN
A JOURNAL OF NEUROLOGY

Dynamic functional reorganization of the motor execution network after stroke

Liang Wang,[1,*] Chunshui Yu,[2,3,*] Hai Chen,[4] Wen Qin,[3] Yong He,[1] Fengmei Fan,[1] Yujin Zhang,[1] Moli Wang,[4] Kuncheng Li,[3] Yufeng Zang,[1] Todd S. Woodward[5] and Chaozhe Zhu[1]

1 State Key Laboratory of Cognitive Neuroscience and Learning, Beijing Normal University, Beijing 100875, People's Republic of China
2 Department of Radiology, Tianjin Medical University General Hospital, Tianjin 300052, People's Republic of China
3 Department of Radiology, Xuanwu Hospital of Capital Medical University, Beijing 100053, People's Republic of China
4 Department of Neurology, Xuanwu Hospital of Capital Medical University, Beijing 100053, People's Republic of China
5 Department of Psychiatry, University of British Columbia, Vancouver, BC V6T 2A1, Canada

*These authors contributed equally to this work.

Correspondence to: Chaozhe Zhu, PhD,
State Key Laboratory of Cognitive Neuroscience and Learning,
Beijing Normal University,
Beijing 100875,
People's Republic of China
E-mail: czzhu@bnu.edu.cn

Numerous studies argue that cortical reorganization may contribute to the restoration of motor function following stroke. However, the evolution of changes during the post-stroke reorganization has been little studied. This study sought to identify dynamic changes in the functional organization, particularly topological characteristics, of the motor execution network during the stroke recovery process. Ten patients (nine male and one female) with subcortical infarctions were assessed by neurological examination and scanned with resting-state functional magnetic resonance imaging across five consecutive time points in a single year. The motor execution network of each subject was constructed using a functional connectivity matrix between 21 brain regions and subsequently analysed using graph theoretical approaches. Dynamic changes in topological configuration of the network during the process of recovery were evaluated by a mixed model. We found that the motor execution network gradually shifted towards a random mode during the recovery process, which suggests that a less optimized reorganization is involved in regaining function in the affected limbs. Significantly increased regional centralities within the network were observed in the ipsilesional primary motor area and contralesional cerebellum, whereas the ipsilesional cerebellum showed decreased regional centrality. Functional connectivity to these brain regions demonstrated consistent alterations over time. Notably, these measures correlated with different clinical variables, which provided support that the findings may reflect the adaptive reorganization of the motor execution network in stroke patients. In conclusion, the study expands our understanding of the spectrum of changes occurring in the brain after stroke and provides a new avenue for investigating lesion-induced network plasticity.

Keywords: stroke; network; small-world; connectivity; functional magnetic resonance imaging

Received August 16, 2009. Revised December 30, 2009. Accepted February 1, 2010

Introduction

Motor deficit is the most prominent symptom in ischaemic stroke, and spontaneous recovery of motor function has been observed during the first several months after stroke onset (Duncan *et al*., 2000). This recovery has been commonly attributed to cortical reorganization, which has been confirmed by the findings from functional neuroimaging studies, including the increased recruitment of contralesional motor areas (Johansen-Berg *et al*., 2002; Small *et al*., 2002; Ward *et al*., 2003; Lotze *et al*., 2006; Calautti *et al*., 2007), increased activity in non-primary motor areas (Chollet *et al*., 1991; Weiller *et al*., 1992; Tombari *et al*., 2004), and the focalization of ipsilesional sensorimotor areas (Feydy *et al*., 2002; Jaillard *et al*., 2005) and language areas (Saur *et al*., 2006). Moreover, the changes in functional and effective connectivity (Friston, 1994), such as increased coherence over the contralesional hemisphere (Gerloff *et al*., 2006), increased task-related corticocortical coupling (Strens *et al*., 2004) and decreased bidirectional coupling between ipsilesional supplementary motor area and primary motor area (Grefkes *et al*., 2008), also imply the existence of the functional reorganization. The cortical reorganization hypothesis is also supported by structural neuroimaging studies, in which the increased cortical thickness in the ipsilesional sensorimotor areas was found (Schaechter *et al*., 2006). In addition, the white matter reorganization has been demonstrated by studies finding increased integrity of whole brain white matter (Wang *et al*., 2006). Despite these advances in the motor-related reorganization literature, little is known about the dynamic changes in the integrative ability of the whole motor network associated with revealed alterations of both local brain activity and functional and anatomical connectivity, which can enhance our understanding of functional reorganization for the motor restoration following stroke.

In recent years, graph theory has been introduced as a novel method or studying functional networks in the central nervous system (for a recent review, see Bullmore and Sporns, 2009). This approach, based on an elegant representation of nodes (vertices) and links (edges) between pairs of nodes, describes important properties of complex systems by quantifying topologies of network representations (Boccaletti *et al*., 2006). Nodes in large-scale brain networks usually represent anatomically defined brain regions, while links represent functional or effective connectivity. Functional connectivity corresponds to magnitudes of temporal correlations in activity (Friston *et al*., 1993) and may occur between pairs of anatomically unconnected regions. Depending on the measure, functional connectivity may reflect linear or nonlinear interactions (Zhou *et al*., 2009), which can be estimated using many methods such as linear correlation (Horwitz *et al*., 1998; Fox *et al*., 2005; Salvador *et al*., 2005), coherence (Sun *et al*., 2004), synchronization likelihood (Stam and van Dijk, 2002), (constrained) principal (Friston *et al*., 1993; Woodward *et al*., 2006) or independent component analysis (McKeown and Sejnowski, 1998) and partial least squares (McIntosh *et al*., 1996). Effective connectivity represents direct or indirect influences that one brain region exerts over another one (Friston, 1994), quantified by various mathematical models, such as structural equation modelling (McIntosh and Gonzalez-Lima, 1994), Granger causality (Roebroeck *et al*., 2005), multivariate autoregressive modelling (Harrison *et al*., 2003), dynamic causal modelling (Friston *et al*., 2003) and Bayesian networks (Zheng and Rajapakse, 2006). The above-mentioned methods can really introduce measures that describe the relationships between nodes. Based on these measures, graph theoretical methods can build abundant models of complex networks to characterize connection patterns within the brain further from a perspective of topological organization. It has been generally believed that functional segregation and integration are two major organizational principles of the human brain. An optimal brain requires a balance between local specialization and global integration of brain functional activity (Tononi *et al*., 1998). This is properly supported by graph indices [e.g. clustering coefficients (an index of functional segregation) and path length (an index of functional integration)] used in the analysis of functional brain networks (Bassett and Bullmore, 2006; Stam and Reijneveld, 2007). The resultant coordinated patterns with high clustering coefficients and short path length, known as a small-world network model (Watts and Strogatz, 1998), reflect the need of the brain networks to satisfy the competitive demands of local and global processing (Kaiser and Hilgetag, 2006). In addition, graph theoretical methods also allow one to evaluate regional centrality in a graph using measures of centrality in contrast to the connectivity methods mentioned above. So far, graph theoretical approaches have been applied to study development (Fair *et al*., 2009; Supekar *et al*., 2009), normal ageing (Achard and Bullmore, 2007; Wu *et al*., 2007; Meunier *et al*., 2009) and neuropsychiatric diseases (for a recent review, see Bassett and Bullmore, 2009). However, no study to date has used this model in an attempt to investigate the possible alterations in the brain functional networks in stroke patients. Moreover, in previous studies the model was mainly used in cross-sectional studies. In the current study, a longitudinal design was employed to examine the changes in the network topological pattern during stroke recovery.

In this study, we focused on the motor execution network, due to the importance of executive function in the process of stroke recovery (Wiese *et al*., 2005). We sought to investigate dynamic changes in the topological patterns of the network during recovery process. The main hypotheses were as follows:

(i) Several recent studies have shown that the brain functional networks shifted towards the topological pattern of random networks in different types of brain pathology, such as brain tumours (Bartolomei *et al*., 2006a), Alzheimer's disease (Stam *et al*., 2009), schizophrenia (Micheloyannis *et al*., 2006; Rubinov *et al*., 2009) and interictal recordings of patients with epilepsy pathological networks (Ponten *et al*., 2007) and severe traumatic brain injury (Nakamura *et al*., 2009). It is possible that network randomization may be a final common pathway for different types of brain damage, resulting from a compensatory but non-optimized outgrowth of new connections because of impaired normal connection pathway. In the current study, we hypothesized that motor network randomization would be observed during stroke recovery.

(ii) Recent longitudinal studies have showed progressive improvement in the ipsilesional primary sensorimotor cortex (Dijkhuizen *et al.*, 2001; Feydy *et al.*, 2002) and increasing brain activity in controlesional cerebellum (Small *et al.*, 2002) after stroke; we hypothesized that gradually increased regional centralities and functional connectivity related to such regions in the network would be observed as time elapsed.

Materials and methods

Participants

Ten right-handed patients (nine male and one female; mean age 48.3 years; range 41–55 years) with left motor pathway subcortical stroke were enrolled from the inpatient services at the Xuanwu Hospital of Capital Medical University (Beijing, China). All participants were first-onset stroke patients and showed motor deficits. None had a history of neurological or psychiatric disorders. Conventional magnetic resonance images (MRI) did not find any abnormalities except for the infarct lesion in each patient. A series of neurological examinations were performed, including the Motricity Index, Modified Rankin Scale, the Barthel Index and the National Institutes of Health Stroke Scale. The patients were scanned and clinically assessed at five time points, i.e. 1 week, 2 weeks, 1 month, 3 months and 1 year after stroke, as current literature suggests that the recovery process after stroke was assumed to consist of three phases (Saur *et al.*, 2006). The clinical characteristics of the stroke patients are summarized in Table 1. Nine age-matched healthy controls (mean age 48.1 years; range 41–53 years) were recruited in a single run to identify the lesion-reduced functional reorganization in patients with stroke at the early acute stage (about 2 weeks after stroke). In addition, to validate whether brain functional networks of controls exhibited stable network topology, two groups of healthy subjects were scanned separately in either a cross-sectional (36 subjects; mean age 53.4 years; range 31–90 years) or longitudinal design (12 subjects; mean age 24.1 years; range 22–29 years), where time points were split into three 1-week intervals. The Ethics Committee of Xuanwu Hospital approved this experiment and each participant gave informed consent.

Table 1 Clinical and demographic data

Patient number	1	2	3	4	5	6	7	8	9	10
Age (years)	42	48	53	52	52	51	43	50	55	41
Gender	M	M	M	F	M	M	M	M	M	M
Localization of infarct	IC CR	IC CR BG	IC CR BG	IC	IC CR BG	IC CR	IC CR	IC CR	IC	IC CR BG
Past medical history	Nil	HT HL	Nil	HT	HT	HT	Nil	HT	HT DT	DT
The number of scans	5	5	5	2	5	5	3	4	3	5
Scan time (day)	4	1	2	2	0	4	1	–	6	4
	13	12	16	12	14	13	9	11	12	13
	32	35	34	–	30	27	–	33	31	29
	147	88	97	–	92	93	–	93	–	111
	354	301	350	–	369	411	300	432	–	375
Motricity Index	33	0	14	14	141	14	28	–	37	0
(0–200)	88	14	58	28	183	37	47	86	53	14
	130	19	88	–	198	47	–	138	91	33
	190	82	113	–	198	88	–	179	–	78
	190	95	113	–	198	116	130	183	–	83
Modified Rankin Scale	5	5	5	5	5	5	5	–	5	5
(0–5)	5	5	4	5	3	5	5	5	5	5
	3	5	3	–	2	4	–	3	4	5
	1	3	3	–	1	3	–	2	–	3
	1	3	3	–	1	1	2	2	–	3
Barthel Index	20	0	20	0	0	10	20	–	25	0
(0–100)	55	25	60	25	85	25	30	15	25	15
	85	35	95	–	90	50	–	70	60	25
	100	80	95	–	100	75	–	100	–	60
	100	85	95	–	100	100	90	100	–	60
National Institutes of Health Stroke Scale	10	14	8	11	5	10	7	–	8	15
(0–15)	3	11	6	6	2	8	5	6	7	13
	2	10	3	–	2	8	–	5	5	13
	0	8	2	–	0	5	–	2	–	6
	0	5	2	–	0	2	1	1	–	6

M = male; F = female; IC = internal capsule; CR = corona radiate; BG = basal ganglia; HT = hypertension; DT = diabetes; HL = hyperlipidaemia; '–' = no functional MRI data.

Data acquisition

All images were acquired on a Siemens Trio 3.0 Tesla MRI scanner (Siemens, Erlangen, Germany) at the Xuanwu Hospital of Capital Medical University. The head of each participant was snugly fixed by foam pads to reduce head movements and scanner noise. All functional magnetic resonance imaging (fMRI) data of the whole brain from the top of the brain to the lower part of the medulla oblongata were acquired using an echo-planar imaging sequence: 32 axial slices, thickness/gap = 3/1 mm, matrix = 64 × 64, repetition time = 2000 ms, echo time = 30 ms, flip angle = 90°, field of view = 220 mm × 220 mm. Structural images were obtained in a sagittal orientation employing a magnetization prepared rapid gradient echo sequence over the whole brain: 176 slices, thickness/gap = 1.0/0 mm, matrix = 256 × 224, repetition time = 1600 ms, echo time = 2.6 ms, flip angle = 9°, field of view = 256 mm × 224 mm. T_2-weighted images were acquired using a turbo-spin-echo sequence: 20 axial slices, thickness/gap = 5/6.5 mm, matrix = 512 × 416, repetition time = 4140 ms, echo time = 92 ms, flip angle = 150°, field of view = 187 mm × 230 mm. During the echo-planar imaging data acquisition, subjects were instructed to keep awake, relax with their eyes closed and remain motionless as much as possible. Each scan lasted for 6 min and 180 image volumes were obtained. For each patient, a different number of scans were performed after stroke. In total, 42 acquisitions (up to five scanning sessions per subject) were collected (Table 1).

Preprocessing of functional MRI data

For the dataset of each subject, the first 10 volumes were discarded to allow for magnetization equilibrium effects and the adaptation of the subjects to the circumstances, leaving 170 volumes for further analysis. The resulting datasets were corrected for delay in slice acquisition and motion using SPM5 (http://www.fil.ion.ucl.ac.uk/spm) software. The realigned images were spatially normalized to the standard space of the Montreal Neurological Institute and smoothed (4 mm isotropic kernel). Finally, temporal filter (0.01–0.1 Hz) was carried out based on an ideal rectangle window filter.

Regions of interest in the motor execution network

In general, most stroke patients suffer from various degrees of motor deficit. The recovery from stroke is a complex process, which has been demonstrated to be associated with functional reorganization across brain areas (for a review, see Calautti and Baron, 2003). Recently, a study has demonstrated functional reorganization of motor execution areas rather than motor preparation areas in post-stroke hemiparesis (Wiese *et al*., 2005). Therefore, in this study, we mainly focused on the dynamic changes in the organization of the motor execution network controlling for the movement of the affected hand (right hand in this study). We selected the regions of interest associated with the motor execution network from our previous work with a simple motor task using the right hand (Jiang *et al*., 2004). The regions of interest included 24 regions, such as left primary motor cortex, bilateral dorsolateral and ventrolateral premotor cortex, bilateral superior parietal lobule, bilateral basal ganglia, bilateral thalamus, anterior inferior cerebellum, postcentral gyrus, dentate nucleus, fusiform gyrus, cuneus cortex and posterolateral cerebellum. Recent studies, however, reported that brain activity in fusiform gyrus, cuneus cortex and posterolateral cerebellum were probably associated with visual representation, motor imagery and instruction events (Allen *et al*., 1997; Hanakawa *et al*., 2008) rather than motor execution. Therefore, these five regions of interest were excluded from the current study. In addition, we made two modifications. First, we separated the supplementary motor area region of interest into two (left and right) in order to study whether these performed different roles during the recovery process. Second, we added the right motor cortex into the studied regions of interest since this region might play a pivotal role in stroke recovery (Calautti and Baron, 2003). The original motor cortex coordinates were modified according to Fink *et al*. (1997) and Ward *et al*.'s (2003) studies to locate accurately onto the motor hand area. Thus, a total of 21 regions of interest were obtained by creating 10 mm diameter spheres around the predefined coordinates (Table 2). In addition, to validate our results independently of the regions of interest selection, we applied the same analysis procedures mentioned below to the motor-related and motor-imagery areas reported in Hanakawa *et al*.'s (2008) study. Notably, from the methodological point of view, this study focused on the functional reorganization on the basis of the changes in topological patterns of coordinated networks, while many previous studies addressed this issue using other approaches focusing on local features, such as brain activity (for a review, see Calautti and Baron, 2003) and functional connectivity (Gerloff *et al*., 2006; Saur *et al*., 2006; Grefkes *et al*., 2008). From a network perspective, the graph theoretical approaches employed in this study were interested in exploring dynamic changes in the topology of network organization during stroke recovery, as opposed to comparing to the methods mentioned above.

Construction of brain functional networks

The time series of all voxels in each region of interest were extracted and averaged to obtain a representative time series. Using a multiple linear regression model, spurious variance of the blood oxygen level dependent signal unlikely reflecting neuronal activity was removed from the mean time series (the dependent variable) by regressing out signal attributable to the six parameters obtained by rigid-body head motion correction (three for translation and three for rotation as predictors). The residuals of this regression were then used to substitute for the raw mean time series of the corresponding regions.

For each scan of every subject, we computed Pearson's correlation coefficients between the time series of all possible pairs of 21 regions, yielding one symmetric correlation matrix (i.e. functional connectivity). The network sparsity (i.e. connection density) was defined as the number of existing connections divided by all of their possible connections (Achard and Bullmore, 2007; Wang *et al*., 2009), and used as a threshold measure to convert each correlation matrix into a graph. For a given sparsity, a data-specific correlation value can be determined and separately used to threshold each correlation matrix. Only those absolute correlation coefficients higher than the threshold value were referred to as edge weights. We repeated the same procedure for all correlation matrices. To assure that the functional connectivity used in this study reflected coupling between regions of interest, we performed statistical tests on the functional connectivity matrix constructed from each participant in each session by using one-sample *t*-tests ($P < 0.01$). The ratios of significant connections to all the possible connections are represented in Supplementary Fig. S1. From this figure, we found that the minimum sparsity was slightly more than 50%. Thus, the sparsity threshold of 0.5 was used to convert connectivity matrices into weighted networks (see supplementary materials for the effect of different sparsity thresholds), which led to all

Table 2 Regions of interest for the motor execution network

ID	Region	Abbreviation	Side	MNI coordinate		
				x	y	z
1	Superior cerebellum	SCb	R	16	−59	−21
2	Primary motor cortex	M1	L	−38	−22	56
3	Primary motor cortex	M1	R	38	−22	56
4	Thalamus	Th	L	−10	−20	11
5	Superior parietal lobule	SPL	L	−22	−62	54
6	Supplementary motor area	SMA	L	−5	−4	57
7	Supplementary motor area	SMA	R	5	−4	57
8	Dorsolateral premotor cortex	PMd	R	28	−10	54
9	Ventrolateral premotor cortex	PMv	L	−49	−1	38
10	Superior cerebellum	SCb	L	−25	−56	−21
11	Superior parietal lobule	SPL	R	16	−66	57
12	Dentate nucleus	DN	R	19	−55	−39
13	Ventrolateral premotor cortex	PMv	R	53	0	25
14	Anterior inferior cerebellum	AICb	L	−22	−45	−49
15	Anterior inferior cerebellum	AICb	R	16	−45	−49
16	Postcentral gyrus	PCG	R	37	−34	53
17	Dorsolateral premotor cortex	PMd	L	−22	−13	57
18	Basal ganglia	BG	R	22	−2	12
19	Basal ganglia	BG	L	−25	−14	8
20	Thalamus	Th	R	7	−20	11
21	Dentate nucleus	DN	L	−28	−55	−43

Note that the regions are selected from a previous study (Jiang *et al*., 2004). We carefully examined the location of each region of interest with a 10 mm diameter sphere and did not observe any overlap between each pair of regions by their Euclidean distance. MNI = Montreal Neurological Institute.

regions of interest included in the network (except 3 sessions of the 42 scanning sessions including 19 regions).

Graph theoretical approaches

Small-world measures of a network (clustering coefficient C_p, and shortest path length L_p) were originally proposed by Watts and Strogatz (1998). Briefly, the C_p is the average of the clustering coefficients over all nodes in a network, which quantifies the extent of local cliquishness or local efficiency of information transfer of a network. The L_p of a network is the average minimum number of connections that link any two nodes of the network, which quantifies the ability of parallel information propagation or global efficiency (Latora and Marchiori, 2001) of a network. Most brain network studies to date have investigated the brain's topological properties by analysing binarized graphs in which every network edge has an equal weight of 1. In this study, we characterized the dynamic changes in the coordinated pattern of motor execution networks by a weighted network analysis approach, which took into account of network edge strength in terms of functional connectivity.

Weighted clustering coefficient

For a weighted graph, the weighted clustering coefficient of a vertex i is defined as (Barrat *et al*., 2004)

$$C_i^w = \frac{1}{s_i(k_i-1)} \Sigma_{(j,k)} \frac{w_{ij}+w_{ik}}{2} a_{ij}a_{ik}a_{jk},$$

where the normalizing factor $s_i(k_i-1)$ [s_i is the strength of the vertex defined as the sum of the weights w_{ij}(the correlation coefficients between regions) of the connected edges: $s_i = \Sigma_j w_{ij}$] assures that $0 \le C_i^w \le 1$; k_i (generally called the node degree) is the number of the edges connected to the node i; a_{ij} is the element of adjacency matrix, which is 1 if there is a edge connecting the node i and node j, otherwise is 0. Thus, the weighted clustering coefficient of a weighted network with N nodes is defined as

$$C^w = \frac{1}{N} \Sigma_{i=N}^{N} C_i^w.$$

Apart from the weighted clustering coefficient, we note that alternative definitions have recently been proposed (Onnela *et al*., 2005; Stam *et al*., 2009).

Weighted shortest path length

The original L_p definition is problematic in graphs that include more than one component. To avoid this situation, L_p is measured here by using an inverse of the harmonic mean of the minimum path length as proposed by Newman (2003). For a weighted graph, the weighted shortest path length is defined as

$$L^w = \frac{N(N-1)}{\Sigma_{i=1}^{N} \Sigma_{j\neq i}^{N} 1/l_{ij}^w}$$

where $l_{ij}^w = \min_{i \Leftrightarrow j}(\mathrm{sum}(d_{ij}))$ and $d_{ij} = 1/w_{ij}$. Here, the shortest weighted path length l_{ij}^w between any pair of node i and j in the graph indicates the minimum value of the sum of transformed weights d_{ij} (i.e. functional distance) over all possible paths. Typically, regular networks are high C^w with large L^w but random networks are low C^w with small L^w. To correct for differences in the mean connection weights across multiple scanning sessions and subjects, we computed the normalized C^w ($Gamma = C^w/C_{rand}^w$) and L^w ($Lambda = L^w/L_{rand}^w$) by comparing C^w and L^w values with the

corresponding index averaged over 50°-matched surrogate networks (Maslov and Sneppen, 2002; Sporns and Zwi, 2004).

Betweenness centrality

In this study, we also analysed nodal (regional) characteristics of the brain network, which were measured by using betweenness centrality (Freeman, 1977)

$$B_i = \Sigma_{s\neq i\neq t}\frac{P_{st}(i)}{P_{st}},$$

where B_i is the betweenness of a node i in the network; $P_{st}(i)$ indicates the number of shortest paths between any two nodes (s and t) that pass through the node i; and P_{st} denotes the total number of shortest paths between the two nodes (s and t). Furthermore, we calculated the normalized betweenness centrality $BC_i = B_i/<B>$ (He *et al.*, 2008), where $<B>$ is the averaged betweenness across all the nodes. As a regional centrality measure, the BC captures the influence of a node over information flow between other nodes in the network.

Statistical analysis

In this study, a linear mixed model was employed to characterize monotonic changes in network parameters (i.e. *gamma, lambda,* betweenness centrality and functional connectivity) over time (or degree of clinical recovery). The random intercept term accounts for the correlation due to repeated measurements within single patient (Gibbons *et al.*, 1988). This model can allow us to use all available data for each patient, even if some time points are missing. Each patient was assumed to possess a common slope (fixed effect) with only the intercepts allowed to vary (random effect). The model was the following:

$$Y_{ij} = \mu + b_i + X_{ij}\beta + \varepsilon_{ij}, \quad i = 1, 2, ..., N,$$

where Y_{ij} is each network parameter from the jth scan (up to five scans) of the ith patient; μ is the intercept term common to all subjects; b_i is a random intercept allowing a unique intercept for each patient; β is the scalar of fixed effect; X_{ij} takes the values x of days post-stroke operated by the exponential function ($e^{-x/\alpha}$) or normalized neurological scores (calculated by subtracting the subject-specific mean from the score of each session), where α is assigned by fitting the normalized Motricity Index scores to the exponential expression, here $\alpha = 29$; N is the number of subjects; and ε_{ij} is the residual error of the model. The model parameters were estimated by the restricted maximum likelihood method and considered significant if the P values were <0.05.

Results

Behavioural data

The mean interval (±standard deviation) from stroke onset to each of the five scans was 2.7 ± 1.9, 12.5 ± 1.8, 31.4 ± 2.7, 103.0 ± 20.7 and 361.5 ± 46.7 days. The lesions were represented by T_2-weighted images in the first session (Fig. 1) and were measured by manually tracing on the T_2-weighted images using MRIcro software (version 1.40, http://www.mricro.com). The mean lesion volume was 11.2 ± 9.5 ml. In this study, of the ten patients, six patients participated in all five functional MRI sessions. For the other participants, the number of scans is shown in Table 1. Based on these subjects, one-way repeated measures analysis of variance (ANOVA) was performed on each of the scales (i.e. Motricity Index, Modified Rankin Scale, the Barthel Index and National Institutes of Health Stroke Scale) and all the results demonstrated significant recovery ($P<0.001$).

Dynamic changes in network topology

The *gamma* and *lambda* quantify the extent of local cliquishness and globally parallel communication of information transfer of a network, respectively, independent of mean connection strength. In this study, the fitted *gamma* (for the actual values, Supplementary Fig. S2) significantly decreased as a function of post-stroke time ($P = 0.011$) after removing the correlation of repeated measurements, whereas the fitted *lambda* exhibited non-significant changes ($P = 0.813$) after removing the correlation due to repeated measurements within each subject (Fig. 2). In addition to sparsity thresholds, we also employed correlation values as thresholds to generate graphs in order to strengthen the reliability of this finding. Supplementary Fig. S3 illustrates the effect of changes in significance levels on *gamma*. We found that *gamma* was still significantly reduced during stroke recovery (see online supplementary materials for details). These findings suggest that over a year of recovery motor execution networks in patients became increasingly random due to lower normalized clustering. Considering that infarct lesion may affect the neurovascular coupling (Murata *et al.*, 2006), we also compared *gamma* and *lambda* in the first session with those obtained from the nine age-matched controls. No significant difference in either *gamma* or *lambda* was observed ($P>0.05$).

We used two groups of healthy subjects to investigate whether the controls showed stable network efficiencies. First, a separate permutation analysis was performed on the group of 36 healthy subjects. From this dataset, we randomly sampled two groups of 10 individuals (in accordance with our study sample size) up to 5000 times. For each sample set, a two-sample t-test was conducted on either *gamma* or *lambda* computed by the same approaches. There were no significant differences in each of the two parameters between any two healthy groups ($P>0.05$). Secondly, one-way repeated measures analyses of variance (ANOVAs) were applied to the network parameters obtained from the control dataset scanned over three time points. Likewise, no significant difference was observed across the different scanning sessions (Supplementary Table S2). Taken together, these findings not only suggest that the analysis of control groups could display stable network topology but also removed the possibility that scanner instability could explain the significant differences in the network indices.

To validate the robustness of our findings, we repeated our analysis on the motor execution network constructed by the motor-related areas as found by Hanakawa *et al.*'s (2008) study. The results from the reconstructed network were consistent with our aforementioned findings, i.e. significant decreases in *gamma* ($P = 0.003$) and *lambda* ($P = 0.014$) over time, suggesting a shift towards random networks. Moreover, the same analysis methods were also applied to the motor-imagery network

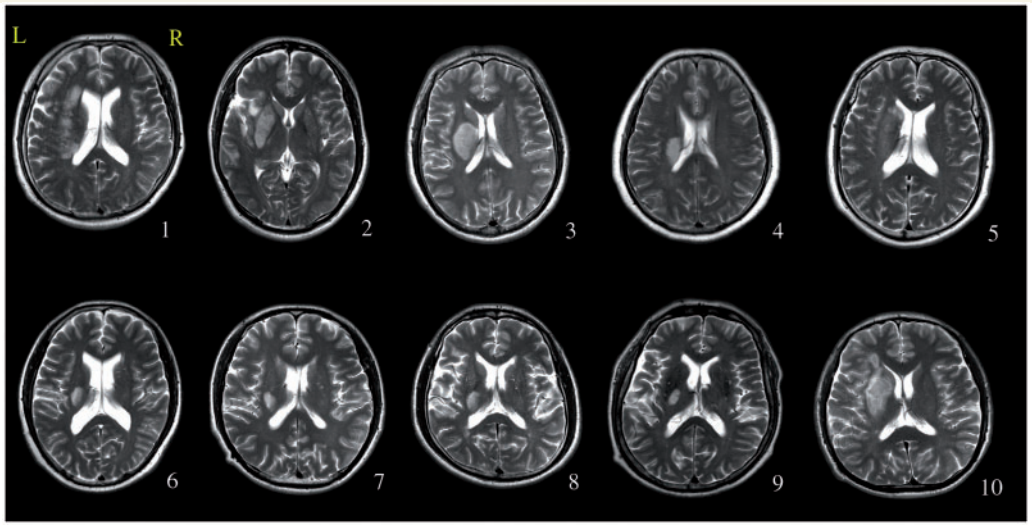

Figure 1 Individual T_2-weighted images in the first session. The panel shows the slice with maximum infarct volume. Each subject is coded by the same serial number as the first row in Table 1.

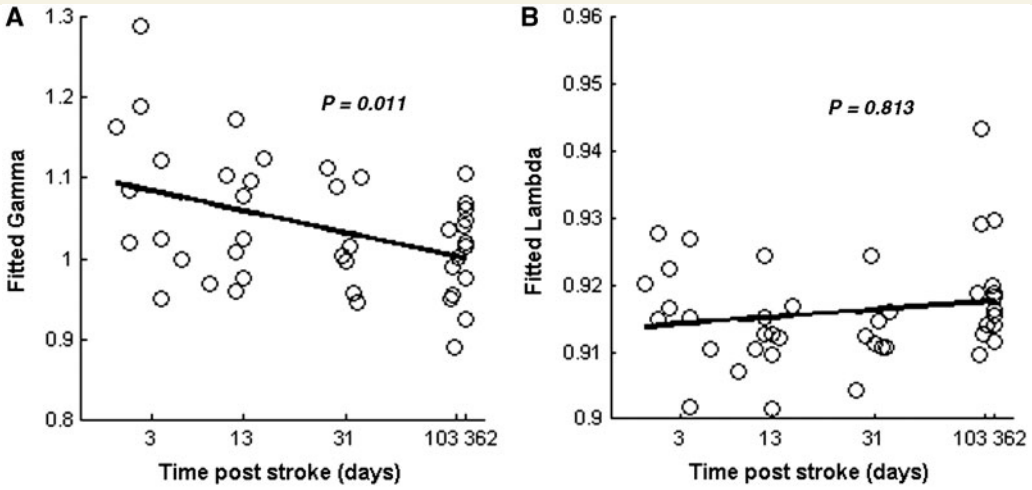

Figure 2 The fitted gamma (**A**) and the lambda (**B**) over time, post-stroke. *Y*-axis values denote the measurements after removing the correlation due to repeated measurements within each subject. The *gamma* significantly declines as a function of time after stroke onset, whereas *lambda* does not change significantly. The abscissa shows the mean scan days after stroke onset (an exponential scale, see the 'Materials and methods' section). Circles show data for individual participants in each session.

obtained from this study (Hanakawa *et al*., 2008). However, no significant changes in *gamma* ($P = 0.3$) and *lambda* ($P = 0.126$) were found in the motor-imagery network. These findings further supported our results that the motor executive network architecture was altered during the stroke recovery process rather than the motor imaginary networks.

Dynamic changes in regional centrality

The regional betweenness centrality is a measure of functional importance of a node by acting as a critical station for information processing; nodes with high connection weights usually have high betweenness centrality. During the process of recovery, significantly increased regional centrality was found in ipsilesional motor cortex ($P = 0.03$) and contralesional dentate nucleus ($P = 0.03$), whereas the decreased centrality was observed in ipsilesional anterior inferior cerebellum ($P = 0.002$) and ipsilesional thalamus ($P = 0.06$) (Table 3), suggesting that ipsilesional primary motor cortex and contralesional cerebellum show increased centrality in the network, while ipsilesional cerebellum and thalamus show decreased centrality. In addition, compared to the nine age-matched controls, a trend towards a significant decrease was detected in the left primary motor cortex ($P = 0.06$) in stroke patients, which may be associated with decreased functional connectivity to the region mentioned below. There was no significant difference in the regional centrality obtained

from healthy controls scanned over three time points by using one-way repeated measures ANOVAs (Supplementary Table S2).

Dynamic changes in functional connectivity

Functional connectivity could reflect the interactions between two remote regions. In this study, several resting state functional connectivities between brain regions showed monotonic changes (Fig. 3). Significantly increased connectivity was observed between ipsilesional motor cortex and contralesional motor areas (i.e. postcentral gyrus, ventrolateral premotor cortex, bilateral dorsolateral premotor cortex and motor cortex), between contralesional dentate nucleus and ipsilesional ventrolateral premotor cortex, and between ipsilesional bilateral dorsolateral premotor cortex and contralesional bilateral superior parietal lobule, while significantly decreased connectivity was detected between ipsilesional bilateral thalamus and contralesional areas (i.e. bilateral dorsolateral premotor cortex, supplementary motor area and bilateral basal ganglia); between ipsilesional anterior inferior cerebellum and contralesional areas (i.e. superior cerebellum and bilateral basal ganglia); and between ipsilesional dentate nucleus and bilateral basal ganglia. The altered functional connectivities to the ipsilesional motor cortex, bilateral thalamus, anterior inferior cerebellum and contralesional dentate nucleus were consistent with these areas representing changed regional centrality mentioned above, providing support of the functional reorganization within the motor network after stroke. Together, these findings suggest an adaptive change of functional connectivity paralleling recovery in patients with stroke. Additionally, in the early acute stage, significantly decreased functional connectivity to the ipsilesional motor cortex and increased functional connectivity to the ipsilesional thalamus and cerebellum were observed compared to the nine age-matched controls (Supplementary Table S3).

Relationship between the network parameters and the clinical measures

In this study, we were also interested in the relationship between the network parameters and the actual recovery rate reflected by neurological examinations in stroke population. The fitted normalized $C^w(gamma)$ significantly correlated with all of the neurological scales during the stroke recovery at the significance level of $P<0.05$ (Table 4). The centralities of several areas were related to these scales, such as ipsilesional motor cortex, supplementary motor area, bilateral thalamus and anterior inferior cerebellum as well as contralesional anterior inferior cerebellum and dentate nucleus. The findings suggest that the network parameter could predict the recovery degree after stroke. From visual inspection of Table 4, the centralities of these areas and *gamma* showed consistent correlations with different neurological examinations. Likewise, the fitted functional connectivity also indicated significant correlations with these examinations (Table 6), which was in accordance with altered functional connectivity over time (Table 5). In addition, the correlations between lesion volumes obtained from the first time point and *gamma* ($r=-0.44$) and *lambda* ($r=0.31$) were observed (Supplementary Fig. S4). Although the correlations did not reach a significant level, possibly due to the small sample size (nine subjects), this finding indicated that a larger lesion volume could possibly disrupt the

Table 3 Altered regional centrality over time ($P<0.05$)

Region	*t*-value	*P*-value
Left primary motor cortex	2.00	0.03
Right dentate nucleus	1.98	0.03
Left supplementary motor area	1.52	0.07*
Left anterior inferior cerebellum	−3.10	0.002
Left thalamus	−1.58	0.06*

The positive *t*-values show increased regional centrality over time in stroke patients. The *P*-values marked by asterisk become marginally significant.

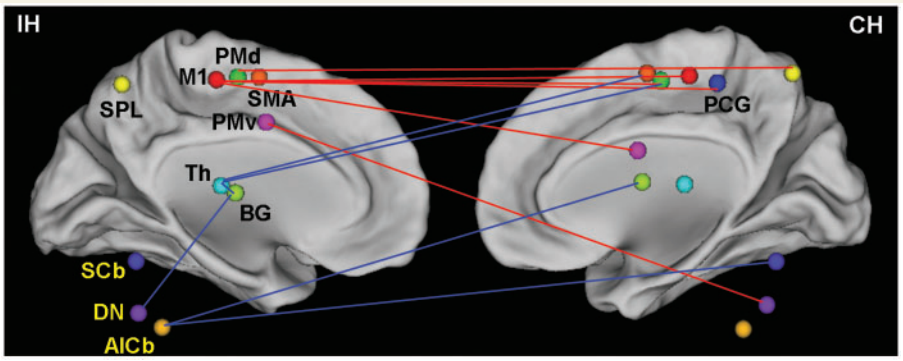

Figure 3 Monotonically increased and decreased functional connectivity over time. All regions of interest (IH, 10 areas; CH, 11 areas) are projected to the medial sagittal section of the fiducial brain using CARET software (http://brainmap.wustl.edu/caret/). The gradually increased connections (red lines) are mainly located between ipsilesional primary cortex area and contralesional key motor areas, whereas the decreased connections (blue lines) involve ipsilesional subcortical areas and cerebellum. Each area is displayed with a unique colour and homologous areas show the same colour. IH = ipsilesional hemisphere; CH = contralesional hemisphere. See Table 2 for the abbreviations of brain regions.

Table 4 The correlation between regional centrality and the clinical measures ($P < 0.05$)

Region	Side	*t*-value	*P*-value	Region	Side	*t*-value	*P*-value
MI (↑↑)				MRS (↓↑)			
SMA	L	1.94	0.03	AICb	L	2.14	0.02
DN	R	1.88	0.04	Th	L	1.42	0.08*
AICb	R	1.80	0.04	DN	R	−1.98	0.03
M1	L	1.58	0.06*	SMA	L	−1.97	0.03
AICb	L	−3.11	0.002	M1	L	−1.76	0.04
Th	L	−1.33	0.09*	AICb	R	−1.36	0.09*
Normalized C^w		−1.95	0.03	Normalized C^w		1.88	0.03
BI (↑↑)				NIHSS (↓↑)			
DN	R	2.30	0.01	AICb	L	3.33	0.001
M1	L	2.00	0.03	Th	L	2.08	0.02
AICb	R	1.79	0.04	M1	L	−2.40	0.01
SMA	L	1.67	0.05	AICb	R	−2.00	0.03
AICb	L	−3.00	0.003	SMA	L	−1.94	0.03
Th	L	−1.70	0.05	DN	R	−1.94	0.03
Normalized C^w		−2.65	0.01	Normalized C^w		2.13	0.02

The double arrows (↑↑) following each neurological scale indicate more scores (the first arrow), more recovery from stroke (the second arrow) and vice versa. Positive *t*-values show positive correlations. Increased regional centrality over time is highlighted by light grey background in stroke patients. The *P*-values marked by asterisk are marginally significant. The normalized L^w measures are not presented due to non-significant correlation. See Table 1 for the neurological scores in detail. See Table 2 for the abbreviations of the regions.

Table 5 Altered functional connectivities over time ($P < 0.01$)

Region	Region	*t*-value	*P*-value
Increased functional connectivity			
Left primary motor cortex	Right postcentral gyrus	3.66	0.001
Left primary motor cortex	Right ventrolateral premotor cortex	3.11	0.002
Right dentate nucleus	Left ventrolateral premotor cortex	2.81	0.004
Left primary motor cortex	Right dorsolateral premotor cortex	2.68	0.006
Left dorsolateral premotor cortex	Right superior parietal lobule	2.66	0.006
Left primary motor cortex	Right primary motor cortex	2.56	0.008
Decreased functional connectivity			
Left thalamus	Right dorsolateral premotor cortex	−3.48	0.001
Left anterior inferior cerebellum	Right superior cerebellum	−3.37	0.001
Left thalamus	Right supplementary motor area	−2.87	0.004
Left thalamus	Left basal ganglia	−2.58	0.008
Left dentate nucleus	Left basal ganglia	−2.48	0.01
Left anterior inferior cerebellum	Right basal ganglia	−2.47	0.01

reorganization pattern of the motor executive networks in terms of decreased *gamma* and increased *lambda*. Similarly, the regional centrality and functional connectivity related to ipsilesional motor cortex and contralesional cerebellum showed significantly positive correlations with stroke recovery scores, whereas these measures related to ipsilesional thalamus and cerebellum showed significantly negative correlations. The specific relations between coordinated network topological patterns and differential behavioural recovery strengthened the putative relation between resting-state brain measures and active behaviours. Also, inadvertent head motion during data acquirement may induce false-positives (Calautti and Baron, 2003). In this study, head motion from the two subjects (1 and 10) at the first session was greater than 3 mm in displace transform compared to other data sets. Though the influence of head motion had been attenuated by a multiple regression model, the two subjects were discarded from the sample for accurate measurements. The resulting data were recomputed and no obvious alterations were obtained for both network parameters and subsequent correlations with behavioural examinations. In addition, to avoid the effect of the parameter α on our results in the mixed regression model, we reset the α range from 20 to 40 corresponding to a range of ∼30% at the upper and lower bounds. All analyses were recomputed and new results were basically similar to the aforementioned results.

Discussion

This study used graph theoretical approaches to investigate functional reorganization of the motor execution network after subcortical motor pathway stroke. We found that the topology of the

Table 6 The correlation between functional connectivity and the clinical measures ($P < 0.01$)

Region	Side	Region	Side	*T*-value	*P*-value	Region	Side	Region	Side	*t*-value	*P*-value
MI (↑↑)						MRS (↓↑)					
M1	L	PCG	R	4.63	<0.001	Th	L	PMd	R	3.77	<0.001
M1	L	PMv	R	3.32	0.001	AICb	L	SCb	R	2.74	0.005
DN	R	PMv	L	3.11	0.002	Th	L	BG	R	2.68	0.006
M1	L	PMd	R	2.84	0.004	DN	L	SCb	R	2.48	0.009
PMd	L	SPL	R	2.66	0.006	M1	L	PCG	R	−4.10	<0.001
PMd	L	PMv	R	2.62	0.007	M1	L	PMv	R	−3.50	<0.001
M1	L	M1	R	2.61	0.007	M1	L	M1	R	−3.14	0.002
Th	L	PMd	R	−3.65	<0.001	PMd	L	SPL	R	−3.03	0.002
DN	L	BG	L	−2.88	0.004	M1	L	PMd	R	−2.61	0.007
Th	L	BG	R	−2.78	0.005						
AICb	L	SCb	R	−2.68	0.006						
BI (↑↑)						NIHSS (↓↑)					
M1	L	PCG	R	3.66	<0.001	Th	L	PMd	R	3.55	<0.001
M1	L	PMv	R	3.17	0.002	Th	L	SMA	R	2.59	0.007
DN	R	PMv	L	3.10	0.002	M1	L	PCG	R	−4.46	<0.001
SMA	L	SCb	R	2.79	0.005	M1	L	M1	R	−3.28	0.001
PMd	L	PMv	R	2.69	0.006	DN	R	PMv	L	−3.04	0.002
M1	L	M1	R	2.63	0.007	M1	L	PMv	R	−2.75	0.005
PMd	L	SPL	R	2.61	0.007	M1	L	PMd	R	−2.63	0.007
PMd	L	M1	R	2.60	0.007	DN	L	SMA	R	−2.60	0.007
Th	L	PMd	R	−3.76	<0.001	DN	L	PCG	R	−2.55	0.008
Th	L	SMA	R	−3.18	0.002						
AICb	L	SCb	R	−2.77	0.005						
SCb	R	SPL	R	−2.67	0.006						

The double arrows (↑↑) following each neurological scale indicate more scores (the first arrow), more recovery from stroke (the second arrow) and vice versa. The positive *t*-values show positive correlations. The increased functional connectivity over time is highlighted by light grey background.

reorganized network in stroke patients showed a gradual shift towards a random mode over time. The betweenness centrality in the ipsilesional motor cortex and contralesional cerebellum as well as functional connectivity to these regions progressively increased during stroke recovery. Moreover, these metrics correlated with different clinical variables and thus served as a predictor of stroke recovery. Collectively, our findings suggest that persistent functional reorganization within the motor network may underlie the motor recovery process after the subcortical motor pathway stroke.

Altered network organization during stroke recovery

An increasing number of studies have utilized graph theory to investigate the effect of lesions on brain functional networks. Recently, De Vico Fallani *et al*. (2007) compared the cortical motor networks obtained from the patients with spinal cord injury with those from controls. Significant increases in the local efficiency but not in the global efficiency were shown in the spinal cord injury group compared to the healthy group, suggesting that the motor networks in patients with spinal cord injury tend to have regular configuration. Bartolomei *et al*. (2006*b*) indicated a tendency for the large-scale functional networks to be close to a random configuration in patients with brain tumours. In the current study, we observed a significant decrease in the normalized clustering coefficients (*gamma*) during the recovery process, but not in the normalized shortest path length (*lambda*), which suggests that the motor network configuration related to the affected hand shifts towards a configuration of random network. Such a shift was in line with changes found in graph theoretical studies of other disorders (Bartolomei *et al*., 2006*a*; Micheloyannis *et al*., 2006; Ponten *et al*., 2007; Rubinov *et al*., 2009; Stam *et al*., 2009). Moreover, we found a correlation between restoration of function and *gamma* values over time, suggesting that the restoration of function was accompanied by a shift towards a non-optimal network configuration. The network randomization may result from random outgrowth of new connections, which have been validated by many studies on stroke (for a review, see Wieloch and Nikolich, 2006). On a cellular level, one of the major regenerative events occurring in the peri-infarct cortex involves axons sprouting new connections and establishing novel projection patterns (Carmichael, 2006, 2008). Meanwhile, stroke induces a unique permissive environment for axonal sprouting, when neurons activate growth-promoting genes in successive waves and many growth-inhibitory molecules are not yet activated (Carmichael, 2006, 2008). Many animal studies have suggested that axonal sprouting after stroke progresses through specific biological time points: trigger (1–3 days after stroke) (Carmichael and Chesselet, 2002), initiation and maintenance (7–14 days after stroke) (Stroemer *et al*., 1995; Leon *et al*., 2000) and maturation (28 days after stroke) phases (Carmichael *et al*., 2001). Moreover, the time points might be prolonged after stroke in the

human brain. In addition, computational neuroscience has indicated that synaptic formation can be described as a process with random outgrowth patterns (Kaiser *et al.*, 2009). This evidence suggests that new axonal outgrowth may partly account for the randomized network organization found in patients during stroke recovery. However, caution must be taken when interpreting the results on this level. Since a few of the patients did show reduced *gamma* within the first 10–14 days after stroke (Fig. 2), the interpretation mentioned above can only, at best, partially account for the results because novel connections could not lead to the changes in the large-scale networks found during this early time period based on the estimated time points mentioned above. Hence, axonal outgrowth may be one reason for network randomization but it cannot be the only one. After stroke, other changes in structural and functional plasticity (Schaechter *et al.*, 2006) may also contribute to the continued randomization of the network configuration.

The outgrowth of new connections may compensate for impaired normal pathways connecting important nodes after the motor pathway stroke, which has been demonstrated by previous evidence. For example, a previous study on animals has demonstrated increased connections from the ventral premotor cortex to the somatosensory cortex in a monkey with an ischaemic lesion to motor cortex (Dancause *et al.*, 2005). Several studies in humans have found that the pre-existing uncrossed corticospinal tract pathways originating from the contralesional hemisphere were recruited to compensate for the damage to the crossed pathways (Ago *et al.*, 2003; Thomas *et al.*, 2005). Moreover, increased recruitment of the undamaged hemisphere was most commonly seen in patients following stroke (Chollet *et al.*, 1991; Weiller *et al.*, 1992; Ward *et al.*, 2003; Tombari *et al.*, 2004; Gerloff *et al.*, 2006). This phenomenon was also confirmed by two other studies. One study found that the disruption of contralesional premotor cortex activity affected the movement ability of the affected hand, especially in patients that demonstrated poor recovery (Johansen-Berg *et al.*, 2002). Another study showed that during performance of complex motor tasks, the disruption of contralesional sensorimotor areas influenced performance even in well-recovered patients (Lotze *et al.*, 2006). Also, the changes in functional connectivity (Table 5) contributed to the topological reorganization of the motor execution network after stroke.

Notably, it seemed counterintuitive to find that compared with normal controls *gamma*, *lambda* and betweenness centrality were not altered in the acute stage after stroke. Recently, a computational model of brain lesions was used to explore how focal brain lesions could affect the overall performance of brain networks in the non-human primate (Honey and Sporns, 2008) and human brain networks (Alstott *et al.*, 2009). These studies indicated that modelling lesions resulted in non-local, disturbed interactions among regions by deleting central nodes (e.g. association cortex) and edges (the corpus callosum connecting bilateral homogenous regions of cortex). In this regard, the different findings in these studies compared to ours may be accounted for by several reasons. First, in our study, patients with subcortical motor pathway stroke were recruited. Such a lesion damages only a few connections (such as the corticospinal tract) within the executive motor network, rather than cutting off all connections, while the two previous studies mentioned above simulated the process of removing edges by cutting off all connections in the corpus callosum. Secondly, it has been suggested that the subcortical infarction may further impair the structural anatomy of the regions of interest (such as the primary motor cortex) through the process of axonal degeneration. Although the two previous studies demonstrated that instantly removing primary cortices would show very little effect on network organization, the effect of any subsequently degenerative changes on network configuration were not investigated in those studies. The longitudinal design of our study complemented these investigations by investigating the dynamic changes in the network structure over the stroke recovery continuum, as many of the apparent contradictions can be explained by the differences in the study design. In the acute stage after stroke, our findings may indicate that the network parameters are not sensitive to the acute, localized subcortical lesions. In this study, the post-stroke time (mean value = 3 days) in the first session may be too short to result in diffusively structural changes, in terms of the notion that the subcortical ischaemic lesions may need a certain amount of time to affect these cortical regions of interest. The preserved structural anatomy may partially account for our findings. In contrast, few altered functional connectivity (Supplementary Table S2) in this stage indeed indicated the appearance of deleterious effect of the lesion. However, the local abnormalities have not spread among the whole network in this time period. As time elapses, the damaged structural anatomy of the regions of interest may induce the deterioration of the network indices and simultaneously affect the reorganization of the network topology mentioned above.

Altered regional centrality during stroke recovery

In this study, as patients demonstrated recovery from stroke, gradual increases in regional centrality were observed in several regions, including the ipsilesional primary motor areas and contralesional dentate nucleus; while the opposite change was seen in ipsilesional anterior inferior cerebellum and ipsilesional thalamus. Basically, increasing importance of ipsilesional primary motor areas in the network may contribute to the gradual recovery of contralesional affected hand in terms of contralateral motor control. Moreover, a recent study using active motor tasks showed the ipsilesional primary sensorimotor cortex progressing focalization (Feydy *et al.*, 2002). Consistent with existing evidence (Dijkhuizen *et al.*, 2001; Small *et al.*, 2002), our findings indicated a general trend for the focusing of the brain activity towards the primary motor area of lesioned hemisphere as time elapses. Recent studies have shown that the cerebellum is exclusively associated with motor actions ipsilateral to the hand movement (Allen *et al.*, 1997; Shibasaki *et al.*, 1993). Imaging studies have shown increased activity in the contralesional cerebellum as the restoration of motor function (Chollet *et al.*, 1991; Weiller *et al.*, 1992; Jaillard *et al.*, 2005). Importantly, a significant positive nonlinear correlation between the activated volume of the contralesional cerebellum and motor performance was reported across four

time points during the recovery from stroke (Small *et al*., 2002); that is to say, the larger the contralesional cerebellum activation, the better the recovery. A more direct role of the contralesional cerebellum for motor recovery was also observed from patients with focal brain lesion in motor learning (Bracha *et al*., 2000; Dong *et al*., 2007).

In addition, the regional centrality of the ipsilesional anterior inferior cerebellum decreased with the stroke duration and significantly correlated with the degree of recovery. In the acute stroke stage, hemiparetic patients cannot move the affected limbs but overuse the unaffected limbs, which may lead to an increase in the centrality of this area in the motor network (Table 3). However, during recovery of motor function of the affected limbs, such over-recruitment could decline and probably resulted in decreases in the centrality of this area over time. This hypothesis is also supported by the negative correlation between the centrality of this area and behavioural recovery as well as the reduced connectivity related to ipsilesional cerebellum (Table 4) in this study. Taken together, to obtain the more recovery after subcortical stroke, the coordinated motor network might evolve to an adaptive, albeit less optimized, topological configuration through modulating the importance of some region.

Altered functional connectivity during stroke recovery

The changes in the topological patterns of the motor execution network were associated with alterations in the strength of each connection. In this study, we found that connectivity between ipsilesional primary motor cortex and contralesional key motor areas (e.g. postcentral gyrus, ventrolateral premotor cortex, bilateral dorsolateral premotor cortex and motor cortex) were significantly increased. Moreover, most of these connectivities significantly correlated with the degree of motor recovery (Table 6), yielding strong relations to behavioural measures. The importance of the ipsilesional primary motor cortex in recovery has been suggested by a previous study (Mima *et al*., 2001), in which the authors found all direct functional connections to muscle after recovery from subcortical stroke originated from the ipsilesional motor cortex. The connectivity between left primary motor areas and right postcentral gyrus was disrupted in the acute stage (Supplementary Table S3) but fully recovered in the chronic stage, and the increased connectivity correlated with the degree of behavioural recovery, which was compatible with a previous study on patients with spatial neglect after stroke (He *et al*., 2007). In stroke patients, recent studies have argued for a beneficial role of the sensorimotor cortex of the contralesional hemisphere on some aspects of effectively recovered motor behaviour (Gerloff *et al*., 2006; Lotze *et al*., 2006). Also, the connectivity related to these areas in the unaffected side may reflect over recruitments of a pre-existing large-scale distributed motor network (Nelles *et al*., 1999; Calautti *et al*., 2001), possibly involving the uncrossed corticospinal tract originated from the contralesional primary motor area. This provides a route by which signals from the undamaged hemisphere could reach the muscles of the affected side of the body (Nathan and Smith, 1973), compensating for damage of the ipsilesional corticospinal tract. Although a significant interaction between the ipsilesional and contralesional primary motor area was detected over time, which was compatible with a recent cross-sectional study that employed a model of effective connectivity (Grefkes *et al*., 2008), our study did not provide further evidence whether such a relation should be categorized as an inhibitory or excitatory connection. Moreover, changes in functional connectivity during stroke recovery did not involve all brain regions to the same extent, suggesting a heterogeneous plasticity of the overall network structure.

We also found that significantly decreased connections after stroke mainly involved subcortical structures (e.g. the thalamus and basal ganglia) and the ipsilesional cerebellum. In this study, the infarct lesion involved the subcortical areas and further disrupted the anatomical connections between these areas and other brain areas, which may result in the reduced connectivity to the areas. The decreased connections with the ipsilesional cerebellum may result from the aberrant over-recruitment in the early acute stage and return to a normal level in the chronic stage. Also, reduction in functional connectivity may be explained by the relatively decreased centrality in the areas (Table 3).

There are some limitations to this study. First, we used a relatively small sample size to characterize the dynamic functional reorganization of the motor execution network from stroke onset to 1 year post-stroke. However, it is unclear how the topology of the network organization changes after 1 year. In future studies, it would be interesting to collect these stroke patients continually and confirm further the clinical usefulness of these findings. Second, in this study, Pearson's correlation was employed to estimate the relationships between brain regions. However, in recent years, computational methods of neuroimaging have made enormous advances and provided various approaches mentioned above to perform the estimation. In future studies, it would be worthwhile to investigate the effect of different methods on topological characteristics of the brain networks in order to understand the relations between the network structure and the processes taking place on these networks better. Third, in this study we indentified dynamic changes of functional network topology in the motor execution networks. However, the function of the brain is always closely associated with its structure (Alstott *et al*., 2009; Honey *et al*., 2009; van den Heuvel *et al*., 2009). A recent study has indicated that disrupted functional connectivity was related to injuries of white matter tracts measured by diffusion tensor imaging (He *et al*., 2007). In future studies it will be vital to investigate whether the functional reorganization shown here is associated with the anatomical changes after stroke. Fourth, the focus on pre-defined regions of interest limited the region and connection set. Recently, several studies reported that the recovery process may be accompanied by 'displaced' activation in a few motor-related regions (Pineiro *et al*., 2001; Calautti *et al*., 2003; Delvaux *et al*., 2003; Carmichael, 2006; Nair *et al*., 2007), which, in this study, may have resulted in the omission of some motor-related regions or the inclusion of some regions that were no longer motor-related following stroke. In general, a motor task may be effective for fully identifying specific regions of interest in individual patients during recovery. In this regard, we previously tried to instruct stroke patients to perform a simple motor task

during the initial scan stage. However, only a subset of the patients was able to perform the task. Therefore, we employed a widely used region of interest approach to construct resting-state functional connectivity networks (Fox *et al*., 2006; Dosenbach *et al*., 2007; He *et al*., 2007; Fair *et al*., 2008, 2009; Church *et al*., 2009). On the other hand, in this study we adopted 10 mm diameter spheres to create the regions of interest, which could reduce this influence of the displacement to a certain extent. In addition to this, 12 mm diameter spheres were also employed to create regions of interest and then the similar results as mentioned above on changes in network parameters were observed, which further validated the reliability of the findings. Although our study did not provide complete coverage of all activated regions, we note that the topological properties of reorganized cortical network are correlated with the clinical variables quantifying functional recovery. Despite that, we cannot absolutely exclude the influence of displaced activation on network parameters. Further studies would be needed to clarify this issue.

In conclusion, to our knowledge, this study is the first to suggest that the topological structure of the motor-related network underwent dynamic reorganization during stroke recovery. However, the reorganized network deviated away from the optimal network architecture. The gradually decreased clustering property is predictive of the restoration of function over time. In addition, the increased betweenness in ipsilesional primary motor cortex and contralesional cerebellum may contribute to stroke recovery. Taken together, the study expands our understanding of the spectrum of changes occurring in the brain after stroke and opens up a new avenue for investigating lesion-induced network plasticity.

Acknowledgements

We thank all the volunteers and patients for their participation in the study, and three anonymous reviewers for their insightful comments and suggestions. We also thank Dr Rajamannar Ramasubbu of University of Calgary for helpful comments.

Funding

National Key Basic Research and Development Program (973) (Grant No 2003CB716101); the Natural Science Foundation of China (Grant Nos 30670601 and 30970773); Program for New Century Excellent Talents in University (NCET-07-0568).

Supplementary material

Supplementary material is available at *Brain* online.

References

Achard S, Bullmore E. Efficiency and cost of economical brain functional networks. PLoS Comput Biol 2007; 3: e17.

Ago T, Kitazono T, Ooboshi H, Takada J, Yoshiura T, Mihara F, et al. Deterioration of pre-existing hemiparesis brought about by subsequent ipsilateral lacunar infarction. J Neurol Neurosurg Psychiatry 2003; 74: 1152–3.

Allen G, Buxton RB, Wong EC, Courchesne E. Attentional activation of the cerebellum independent of motor involvement. Science 1997; 275: 1940–3.

Alstott J, Breakspear M, Hagmann P, Cammoun L, Sporns O. Modeling the impact of lesions in the human brain. PLoS Comput Biol 2009; 5: e1000408.

Barrat A, Barthelemy M, Pastor-Satorras R, Vespignani A. The architecture of complex weighted networks. Proc Natl Acad Sci USA 2004; 101: 3747–52.

Bartolomei F, Bosma I, Klein M, Baayen JC, Reijneveld JC, Postma TJ, et al. Disturbed functional connectivity in brain tumour patients: evaluation by graph analysis of synchronization matrices. Clin Neurophysiol 2006a; 117: 2039–49.

Bartolomei F, Bosma I, Klein M, Baayen JC, Reijneveld JC, Postma TJ, et al. How do brain tumors alter functional connectivity? A magnetoencephalography study. Ann Neurol 2006b; 59: 128–38.

Bassett DS, Bullmore E. Small-world brain networks. Neuroscientist 2006; 12: 512–23.

Bassett DS, Bullmore ET. Human brain networks in health and disease. Curr Opin Neurol 2009; 22: 340–7.

Boccaletti S, Latora V, Moreno Y, Chavez M, Hwang DU. Complex networks: structure and dynamics. Phys Rep 2006; 424: 175–308.

Bracha V, Zhao L, Irwin KB, Bloedel JR. The human cerebellum and associative learning: dissociation between the acquisition, retention and extinction of conditioned eyeblinks. Brain Res 2000; 860: 87–94.

Bullmore E, Sporns O. Complex brain networks: graph theoretical analysis of structural and functional systems. Nat Rev Neurosci 2009; 10: 186–98.

Calautti C, Baron JC. Functional neuroimaging studies of motor recovery after stroke in adults: a review. Stroke 2003; 34: 1553–66.

Calautti C, Leroy F, Guincestre JY, Baron JC. Dynamics of motor network overactivation after striatocapsular stroke: a longitudinal PET study using a fixed-performance paradigm. Stroke 2001; 32: 2534–42.

Calautti C, Leroy F, Guincestre JY, Baron JC. Displacement of primary sensorimotor cortex activation after subcortical stroke: a longitudinal PET study with clinical correlation. Neuroimage 2003; 19: 1650–4.

Calautti C, Naccarato M, Jones PS, Sharma N, Day DD, Carpenter AT, et al. The relationship between motor deficit and hemisphere activation balance after stroke: a 3T fMRI study. Neuroimage 2007; 34: 322–31.

Carmichael ST. Cellular and molecular mechanisms of neural repair after stroke: making waves. Ann Neurol 2006; 59: 735–42.

Carmichael ST. Themes and strategies for studying the biology of stroke recovery in the poststroke epoch. Stroke 2008; 39: 1380–8.

Carmichael ST, Chesselet M-F. Synchronous neuronal activity is a signal for axonal sprouting after cortical lesions in the adult. J Neurosci 2002; 22: 6062–70.

Carmichael ST, Wei L, Rovainen CM, Woolsey TA. New patterns of intracortical projections after focal cortical stroke. Neurobiol Dis 2001; 8: 910–22.

Chollet F, DiPiero V, Wise RJ, Brooks DJ, Dolan RJ, Frackowiak RS. The functional anatomy of motor recovery after stroke in humans: a study with positron emission tomography. Ann Neurol 1991; 29: 63–71.

Church JA, Fair DA, Dosenbach NU, Cohen AL, Miezin FM, Petersen SE, et al. Control networks in paediatric Tourette syndrome show immature and anomalous patterns of functional connectivity. Brain 2009; 132: 225–38.

Dancause N, Barbay S, Frost SB, Plautz EJ, Chen D, Zoubina EV, et al. Extensive cortical rewiring after brain injury. J Neurosci 2005; 25: 10167–79.

De Vico Fallani F, Astolfi L, Cincotti F, Mattia D, Marciani MG, Salinari S, et al. Cortical functional connectivity networks in normal and spinal cord injured patients: evaluation by graph analysis. Hum Brain Mapp 2007; 28: 1334–46.

Delvaux V, Alagona G, Gerard P, De Pasqua V, Pennisi G, de Noordhout AM. Post-stroke reorganization of hand motor area: a

1-year prospective follow-up with focal transcranial magnetic stimulation. Clin Neurophysiol 2003; 114: 1217–25.
Dijkhuizen RM, Ren J, Mandeville JB, Wu O, Ozdag FM, Moskowitz MA, et al. Functional magnetic resonance imaging of reorganization in rat brain after stroke. Proc Natl Acad Sci USA 2001; 98: 12766–71.
Dong Y, Winstein CJ, Albistegui-DuBois R, Dobkin BH. Evolution of FMRI activation in the perilesional primary motor cortex and cerebellum with rehabilitation training-related motor gains after stroke: a pilot study. Neurorehabil Neural Repair 2007; 21: 412–28.
Dosenbach NU, Fair DA, Miezin FM, Cohen AL, Wenger KK, Dosenbach RA, et al. Distinct brain networks for adaptive and stable task control in humans. Proc Natl Acad Sci USA 2007; 104: 11073–8.
Duncan PW, Min Lai S, Keighley J. Defining post-stroke recovery: implications for design and interpretation of drug trials. Neuropharmacology 2000; 39: 835–41.
Fair DA, Cohen AL, Dosenbach NU, Church JA, Miezin FM, Barch DM, et al. The maturing architecture of the brain's default network. Proc Natl Acad Sci USA 2008; 105: 4028–32.
Fair DA, Cohen AL, Power JD, Dosenbach NU, Church JA, Miezin FM, et al. Functional brain networks develop from a ''local to distributed'' organization. PLoS Comput Biol 2009; 5: e1000381.
Feydy A, Carlier R, Roby-Brami A, Bussel B, Cazalis F, Pierot L, et al. Longitudinal study of motor recovery after stroke: recruitment and focusing of brain activation. Stroke 2002; 33: 1610–7.
Fink GR, Frackowiak RS, Pietrzyk U, Passingham RE. Multiple nonprimary motor areas in the human cortex. J Neurophysiol 1997; 77: 2164–74.
Fox MD, Corbetta M, Snyder AZ, Vincent JL, Raichle ME. Spontaneous neuronal activity distinguishes human dorsal and ventral attention systems. Proc Natl Acad Sci USA 2006; 103: 10046–51.
Fox MD, Snyder AZ, Vincent JL, Corbetta M, Van Essen DC, Raichle ME. The human brain is intrinsically organized into dynamic, anticorrelated functional networks. Proc Natl Acad Sci USA 2005; 102: 9673–8.
Freeman LC. A set of measures of centrality based on betweenness. Sociometry 1977; 40: 35–41.
Friston K. Functional and effective connectivity in neuroimaging: a synthesis. Hum Brain Mapp 1994; 2: 56–78.
Friston KJ, Frith CD, Liddle PF, Frackowiak RS. Functional connectivity: the principal-component analysis of large (PET) data sets. J Cereb Blood Flow Metab 1993; 13: 5–14.
Friston KJ, Harrison L, Penny W. Dynamic causal modelling. Neuroimage 2003; 19: 1273–302.
Gerloff C, Bushara K, Sailer A, Wassermann EM, Chen R, Matsuoka T, et al. Multimodal imaging of brain reorganization in motor areas of the contralesional hemisphere of well recovered patients after capsular stroke. Brain 2006; 129: 791–808.
Gibbons RD, Hedeker D, Waternaux C, Davis JM. Random regression models: a comprehensive approach to the analysis of longitudinal psychiatric data. Psychopharmacol Bull 1988; 24: 438–43.
Grefkes C, Nowak DA, Eickhoff SB, Dafotakis M, Kust J, Karbe H, et al. Cortical connectivity after subcortical stroke assessed with functional magnetic resonance imaging. Ann Neurol 2008; 63: 236–46.
Hanakawa T, Dimyan MA, Hallett M. Motor planning, imagery, and execution in the distributed motor network: a time-course study with functional MRI. Cereb Cortex 2008; 18: 2775–88.
Harrison L, Penny WD, Friston K. Multivariate autoregressive modeling of fMRI time series. Neuroimage 2003; 19: 1477–91.
He BJ, Snyder AZ, Vincent JL, Epstein A, Shulman GL, Corbetta M. Breakdown of functional connectivity in frontoparietal networks underlies behavioral deficits in spatial neglect. Neuron 2007; 53: 905–18.
He Y, Chen Z, Evans A. Structural insights into aberrant topological patterns of large-scale cortical networks in Alzheimer's disease. J Neurosci 2008; 28: 4756–66.
Honey CJ, Sporns O. Dynamical consequences of lesions in cortical networks. Hum Brain Mapp 2008; 29: 802–9.
Honey CJ, Sporns O, Cammoun L, Gigandet X, Thiran JP, Meuli R, et al. Predicting human resting-state functional connectivity from structural connectivity. Proc Natl Acad Sci USA 2009; 106: 2035–40.
Horwitz B, Rumsey JM, Donohue BC. Functional connectivity of the angular gyrus in normal reading and dyslexia. Proc Natl Acad Sci USA 1998; 95: 8939–44.
Jaillard A, Martin CD, Garambois K, Lebas JF, Hommel M. Vicarious function within the human primary motor cortex? A longitudinal fMRI stroke study. Brain 2005; 128: 1122–38.
Jiang T, He Y, Zang Y, Weng X. Modulation of functional connectivity during the resting state and the motor task. Hum Brain Mapp 2004; 22: 63–71.
Johansen-Berg H, Rushworth MF, Bogdanovic MD, Kischka U, Wimalaratna S, Matthews PM. The role of ipsilateral premotor cortex in hand movement after stroke. Proc Natl Acad Sci USA 2002; 99: 14518–23.
Kaiser M, Hilgetag CC. Nonoptimal component placement, but short processing paths, due to long-distance projections in neural systems. PLoS Comput Biol 2006; 2: e95.
Kaiser M, Hilgetag CC, van Ooyen A. A simple rule for axon outgrowth and synaptic competition generates realistic connection lengths and filling fractions. Cereb Cortex 2009; 19: 3001–10.
Latora V, Marchiori M. Efficient behavior of small-world networks. Phys Rev Lett 2001; 87: 198701.
Leon S, Yin Y, Nguyen J, Irwin N, Benowitz LI. Lens injury stimulates axon regeneration in the mature rat optic nerve. J Neurosci 2000; 20: 4615–26.
Lotze M, Markert J, Sauseng P, Hoppe J, Plewnia C, Gerloff C. The role of multiple contralesional motor areas for complex hand movements after internal capsular lesion. J Neurosci 2006; 26: 6096–102.
Maslov S, Sneppen K. Specificity and stability in topology of protein networks. Science 2002; 296: 910–3.
McIntosh AR, Bookstein FL, Haxby JV, Grady CL. Spatial pattern analysis of functional brain images using partial least squares. Neuroimage 1996; 3: 143–57.
McIntosh AR, Gonzalez-Lima F. Structural equation modeling and its application to network analysis in functional brain imaging. Hum Brain Mapp 1994; 2: 2–22.
McKeown MJ, Sejnowski TJ. Independent component analysis of fMRI data: examining the assumptions. Hum Brain Mapp 1998; 6: 368–72.
Meunier D, Achard S, Morcom A, Bullmore E. Age-related changes in modular organization of human brain functional networks. Neuroimage 2009; 44: 715–23.
Micheloyannis S, Pachou E, Stam CJ, Breakspear M, Bitsios P, Vourkas M, et al. Small-world networks and disturbed functional connectivity in schizophrenia. Schizophr Res 2006; 87: 60–6.
Mima T, Toma K, Koshy B, Hallett M. Coherence between cortical and muscular activities after subcortical stroke. Stroke 2001; 32: 2597–601.
Murata Y, Sakatani K, Hoshino T, Fujiwara N, Kano T, Nakamura S, et al. Effects of cerebral ischemia on evoked cerebral blood oxygenation responses and BOLD contrast functional MRI in stroke patients. Stroke 2006; 37: 2514–20.
Nair DG, Hutchinson S, Fregni F, Alexander M, Pascual-Leone A, Schlaug G. Imaging correlates of motor recovery from cerebral infarction and their physiological significance in well-recovered patients. Neuroimage 2007; 34: 253–63.
Nakamura T, Hillary FG, Biswal BB. Resting network plasticity following brain injury. PLoS One 2009; 4: e8220.
Nathan PW, Smith MC. Effects of two unilateral cordotomies on the motility of the lower limbs. Brain 1973; 96: 471–94.
Nelles G, Spiekramann G, Jueptner M, Leonhardt G, Muller S, Gerhard H, et al. Evolution of functional reorganization in hemiplegic stroke: a serial positron emission tomographic activation study. Ann Neurol 1999; 46: 901–9.
Newman MEJ. The structure and function of complex networks. SIAM Rev 2003; 45: 167–256.

Onnela JP, Saramaki J, Kertesz J, Kaski K. Intensity and coherence of motifs in weighted complex networks. Phys Rev E Stat Nonlin Soft Matter Phys 2005; 71: 065103.

Pineiro R, Pendlebury S, Johansen-Berg H, Matthews PM. Functional MRI detects posterior shifts in primary sensorimotor cortex activation after stroke: evidence of local adaptive reorganization? Stroke 2001; 32: 1134–9.

Ponten SC, Bartolomei F, Stam CJ. Small-world networks and epilepsy: graph theoretical analysis of intracerebrally recorded mesial temporal lobe seizures. Clin Neurophysiol 2007; 118: 918–27.

Roebroeck A, Formisano E, Goebel R. Mapping directed influence over the brain using Granger causality and fMRI. Neuroimage 2005; 25: 230–42.

Rubinov M, Knock SA, Stam CJ, Micheloyannis S, Harris AW, Williams LM, et al. Small-world properties of nonlinear brain activity in schizophrenia. Hum Brain Mapp 2009; 30: 403–16.

Salvador R, Suckling J, Coleman MR, Pickard JD, Menon D, Bullmore E. Neurophysiological architecture of functional magnetic resonance images of human brain. Cereb Cortex 2005; 15: 1332–42.

Saur D, Lange R, Baumgaertner A, Schraknepper V, Willmes K, Rijntjes M, et al. Dynamics of language reorganization after stroke. Brain 2006; 129: 1371–84.

Schaechter JD, Moore CI, Connell BD, Rosen BR, Dijkhuizen RM. Structural and functional plasticity in the somatosensory cortex of chronic stroke patients. Brain 2006; 129: 2722–33.

Shibasaki H, Sadato N, Lyshkow H, Yonekura Y, Honda M, Nagamine T, et al. Both primary motor cortex and supplementary motor area play an important role in complex finger movement. Brain 1993; 116: 1387–98.

Small SL, Hlustik P, Noll DC, Genovese C, Solodkin A. Cerebellar hemispheric activation ipsilateral to the paretic hand correlates with functional recovery after stroke. Brain 2002; 125: 1544–57.

Sporns O, Zwi JD. The small world of the cerebral cortex. Neuroinformatics 2004; 2: 145–62.

Stam CJ, de Haan W, Daffertshofer A, Jones BF, Manshanden I, van Cappellen van Walsum AM, et al. Graph theoretical analysis of magnetoencephalographic functional connectivity in Alzheimer's disease. Brain 2009; 132: 213–24.

Stam CJ, Reijneveld JC. Graph theoretical analysis of complex networks in the brain. Nonlinear Biomed Phys 2007; 1: 3.

Stam CJ, van Dijk BW. Synchronization likelihood: an unbiased measure of generalized synchronization in multivariate data sets. Physica D Nonlinear Phen 2002; 163: 236–51.

Strens LH, Asselman P, Pogosyan A, Loukas C, Thompson AJ, Brown P. Corticocortical coupling in chronic stroke: its relevance to recovery. Neurology 2004; 63: 475–84.

Stroemer RP, Kent TA, Hulsebosch CE. Neocortical neural sprouting, synaptogenesis, and behavioral recovery after neocortical infarction in rats. Stroke 1995; 26: 2135–44.

Sun FT, Miller LM, D'Esposito M. Measuring interregional functional connectivity using coherence and partial coherence analyses of fMRI data. Neuroimage 2004; 21: 647–58.

Supekar K, Musen M, Menon V. Development of large-scale functional brain networks in children. PLoS Biol 2009; 7: e1000157.

Thomas B, Eyssen M, Peeters R, Molenaers G, Van Hecke P, De Cock P, et al. Quantitative diffusion tensor imaging in cerebral palsy due to periventricular white matter injury. Brain 2005; 128: 2562–77.

Tombari D, Loubinoux I, Pariente J, Gerdelat A, Albucher JF, Tardy J, et al. A longitudinal fMRI study: in recovering and then in clinically stable sub-cortical stroke patients. Neuroimage 2004; 23: 827–39.

Tononi G, Edelman GM, Sporns O. Complexity and coherency: integrating information in the brain. Trends Cogn Sci 1998; 2: 474–84.

van den Heuvel MP, Mandl RC, Kahn RS, Hulshoff Pol HE. Functionally linked resting-state networks reflect the underlying structural connectivity architecture of the human brain. Hum Brain Mapp 2009; 30: 3127–41.

Wang C, Stebbins GT, Nyenhuis DL, deToledo-Morrell L, Freels S, Gencheva E, et al. Longitudinal changes in white matter following ischemic stroke: a three-year follow-up study. Neurobiol Aging 2006; 27: 1827–33.

Wang L, Zhu C, He Y, Zang Y, Cao Q, Zhang H, et al. Altered small-world brain functional networks in children with attention-deficit/hyperactivity disorder. Hum Brain Mapp 2009; 30: 638–49.

Ward NS, Brown MM, Thompson AJ, Frackowiak RS. Neural correlates of motor recovery after stroke: a longitudinal fMRI study. Brain 2003; 126: 2476–96.

Watts DJ, Strogatz SH. Collective dynamics of 'small-world' networks. Nature 1998; 393: 440–2.

Weiller C, Chollet F, Friston KJ, Wise RJ, Frackowiak RS. Functional reorganization of the brain in recovery from striatocapsular infarction in man. Ann Neurol 1992; 31: 463–72.

Wieloch T, Nikolich K. Mechanisms of neural plasticity following brain injury. Curr Opin Neurobiol 2006; 16: 258–64.

Wiese H, Stude P, Sarge R, Nebel K, Diener HC, Keidel M. Reorganization of motor execution rather than preparation in post-stroke hemiparesis. Stroke 2005; 36: 1474–9.

Woodward TS, Cairo TA, Ruff CC, Takane Y, Hunter MA, Ngan ET. Functional connectivity reveals load dependent neural systems underlying encoding and maintenance in verbal working memory. Neuroscience 2006; 139: 317–25.

Wu T, Zang Y, Wang L, Long X, Hallett M, Chen Y, et al. Aging influence on functional connectivity of the motor network in the resting state. Neurosci Lett 2007; 422: 164–8.

Zheng X, Rajapakse JC. Learning functional structure from fMR images. Neuroimage 2006; 31: 1601–13.

Zhou D, Thompson WK, Siegle G. MATLAB toolbox for functional connectivity. Neuroimage 2009; 47: 1590–607.